ACS Chemical Neuroscience

Research Article

pubs.acs.org/chemneuro

Role of an Absolutely Conserved Tryptophan Pair in the Extracellular Domain of Cys-Loop Receptors

Nina Braun,[†] Timothy Lynagh,[†] Rilei Yu,[‡,§] Philip C. Biggin,[‡] and Stephan A. Pless*[,†]

[†]Department of Drug Design and Pharmacology, University of Copenhagen, Copenhagen 2100, Denmark

[‡]Department of Biochemistry, University of Oxford, South Parks Road, Oxford OX1 3QU, United Kingdom

Supporting Information

ABSTRACT: Cys-loop receptors mediate fast synaptic transmission in the nervous system, and their dysfunction is associated with a number of diseases. While some sequence variability is essential to ensure specific recognition of a chemically diverse set of ligands, other parts of the underlying amino acid sequences show a high degree of conservation, possibly to preserve the overall structural fold across the protein family. In this study, we focus on the only two absolutely conserved residues across the Cys-loop receptor family, two Trp side chains in the WXD motif of Loop D and in the WXPD motif of Loop A. Using a combination of conventional mutagenesis, unnatural amino acid incorporation, immunohistochemistry and MD simulations, we demonstrate the crucial contributions of these two Trp residues to receptor expression and function in two prototypical Cys-loop receptors, the anion-selective GlyR α1 and the cation-selective nAChR α7. Specifically, our results rule out possible electrostatic contributions of these Trp side chains and instead suggest that the overall size and shape of this aromatic pair is required in stabilizing the Cys-loop receptor extracellular domain.

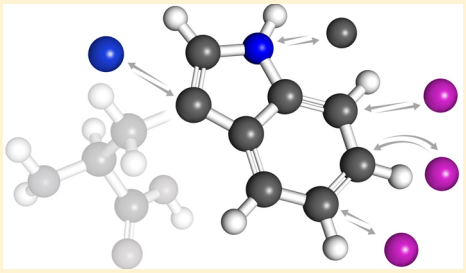

KEYWORDS: *Cys-loop receptors, unnatural amino acids, structure−function, tryptophan cluster, glycine receptor, nicotinic acetylcholine receptor*

Fast synaptic transmission is mediated by ligand-gated ion channels.[1] In vertebrates, most excitatory signals are elicited by cation-selective tetrameric glutamate receptors or pentameric Cys-loop receptors, such as the nicotinic acetylcholine and 5-hydroxytryptamine receptors (nAChRs and 5-HT_3Rs). Conversely, most inhibitory signals are mediated by anion-selective Cys-loop receptors for γ-aminobutyric acid and glycine ($GABA_A$Rs and GlyRs).[2] The important physiological and pharmacological roles of Cys-loop receptors are underscored by the diseases linked to mutations in these membrane proteins[3,4] and the fact that both frontline medicines and deadly neurotoxins act by modulating Cys-loop receptor function.[5,6]

All members of the Cys-loop receptor family share a common architecture, in which a symmetrical arrangement of five subunits establishes a central, ion-conducting pore. Each subunit comprises an extracellular domain (ECD), with a core of 10 β-strands forming a β-sandwich, and a transmembrane domain (TMD) with 4 membrane-spanning helices (M1−M4), of which the M2 helices line the pore.[2] At the extracellular interfaces between adjacent subunits, an arrangement of loops A−C on the principal face and loops D−G on the complementary face forms the agonist-binding sites. Although the overall structure of this large receptor family has been accepted for over a decade,[7−9] detailed investigation is still required to understand how these proteins diverge in ligand recognition and signaling yet still maintain a common structural scaffold. This is of particular importance with regard to our understanding of disease-causing mutations and, ultimately, the ability to create new and highly specific drugs. A surge in structural data has recently greatly aided progress in the field, with numerous X-ray and cryo-electron microscopic structures of mammalian Cys-loop receptors now allowing unprecedented insight into the structural features of this large receptor family.[10−15] It is clear that, in order to accommodate for a wide variety of chemically diverse ligands, different Cys-loop receptors have to display some sequence variability.[16] By contrast, as predicted by the high structural homology, other parts of the underlying amino acid sequences need to show a higher degree of conservation in order to preserve a similar structural fold across the protein family. Here, we set out to determine some of the key structural features that form the main components of this common structural theme. To this end, we focused on the only two absolutely conserved amino acids in 187 functional Cys-loop receptor subunits (or related proteins), a Trp in the Trp-X-Asp ("WXD") motif in loop D and a Trp in the Trp-X-Pro-Asp ("WXPD") motif in loop A (Figure 1). Although both loops contain residues that directly bind agonists, these Trp side chains face away from and are thus unlikely to directly interact with the agonist, according to high-resolution structural data on Cys-loop receptors.[13,17] A special role of these side chains is implicated by the occurrence

Received: November 13, 2015
Accepted: January 14, 2016
Published: January 14, 2016

DOI: 10.1021/acschemneuro.5b00298
ACS Chem. Neurosci. 2016, 7, 339−348

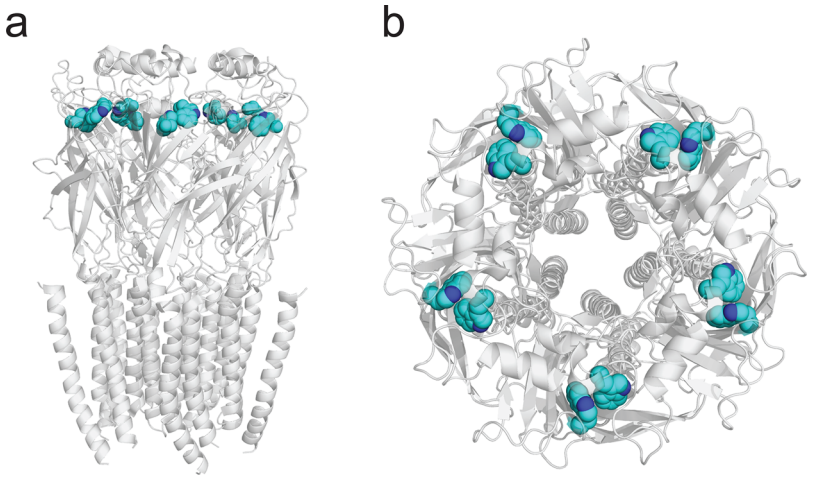

Figure 1. Location of the two conserved Trp residues within the overall Cys-loop receptor structure. Side (a) and top (b) view of the α1 GlyR structure (PDB: 3JAE) with the two Trp side chains highlighted in cyan/blue.

of a Trp-to-Cys mutation at the Loop D position in a human family with hyperekplexia,[18] a rare genetic disease linked to GlyR malfunction and characterized by hypertonia and startle responses to innocuous stimuli.[19] Furthermore, it has been shown in homomeric GlyRs and 5-HT_3Rs and in heteromeric $GABA_A$Rs that receptors bearing conventional mutations at these positions are not targeted to the cell surface.[18−20] These data confirm a role for the conserved Trp residues in receptor expression, but the large structural and chemical differences between tryptophan and conventional substituents (such as phenylalanine, cysteine and glycine employed in those studies) precludes a mechanistic or chemical explanation of exactly how tryptophan achieves this role. Furthermore, the fact that conventional mutations abolish cell surface expression means that the role of these Trp residues in the function of mature receptors alludes us.

Utilizing both anion- and cation-selective homomeric Cys-loop receptors, the glycine receptor α1 (GlyR α1) and the nicotinic acetylcholine receptor α7 (nAChR α7), we employed conventional mutagenesis and immunohistochemistry to establish the requirement of these uniquely conserved Trp residues for functional receptor expression. To more subtly probe for a role of Trp side chains in the function of mature receptors, we measured ligand-gated GlyR and nAChR activation upon incorporation of unnatural amino acids and conducted molecular dynamics simulations of wild-type (WT) GlyRs. Our results rule out possible cation-π interactions with these Trp side chains[21] and instead suggest that the overall size and shape of this aromatic pair is required in stabilizing the top of the Cys-loop receptor ECD.

RESULTS AND DISCUSSION

Two Absolutely Conserved Trp Side Chains. To determine which side chains show the highest degree of conservation across a wide range of different Cys-loop receptors, we aligned the amino acid sequences of 187 subunits known to form functional receptors, including two that lack the TMD (acetylcholine-binding proteins, AChBPs) and two that lack the eponymous Cys-loop (ELIC and GLIC). Intriguingly, we found that among all sequences, the only side chains that were absolutely conserved were the Trp of the Loop D WXD motif and the Trp of the Loop A WXPD motif (Figure 2). Although the Loop D Asp and the Loop A Pro and Asp side chains within these motifs also show a high degree of conservation (Figure 2a), the only residues to be found in every single one of the sequences were the two Trp side chains (Figure S1, Supporting Information). Figure 2b highlights the position of the two Trp residues in the context of their primary structure for a selection of well-known receptors. Although proximal residues are crucial to ligand recognition (reviewed in ref 16), the role of these Trp residues is unknown, despite recent evidence implicating the Loop D Trp in assembly of GlyRs.[18]

A Role for Conserved Trp Side Chains in GlyR Expression. The absolute conservation of the Loop D and Loop A Trp residues implicates these side chains in some crucial role in Cys-loop receptor function. To test for such a role, we turned to the GlyR α1, a prototypical anion-selective member of the family, and introduced a series of mutations at both of these positions. Thus, we generated four mutant GlyRs, Trp68Phe and Trp68Leu (Loop D) and Trp94Phe and Trp94Leu (Loop A), expressed these in *Xenopus laevis* oocytes and measured for responses to application of glycine. Intact responses to glycine in each mutant would suggest that only the hydrophobic character is important, whereas intact responses to glycine only with the Phe substitution would implicate the aromatic nature of the Trp side chains. As expected, WT GlyR α1 responded to glycine concentrations in the low micromolar range (Figure 3a), whereas all mutations abolished any response to glycine, even at very high (100 mM) concentrations (Figure 3b). Impaired GlyR α1 subunit function may be rescued by coexpression with WT β subunits, as shown for α1 mutations linked to hyperekplexia.[22] To test if the GlyR β subunits could restore functional expression to Trp68Leu/Phe or the Trp94Leu/Phe mutants, we coinjected oocytes with mutant GlyR α1 RNA and an excess of GlyR β RNA (which alone does not form functional channels[23]). However, none of these mutant receptors responded to glycine application, suggesting that Trp68Leu/Phe and Trp94Leu/Phe α1 subunits can form neither functional homomers alone nor heteromers with the GlyR β subunit (Figure 3c).

So far, our results suggested that the mutations altered receptors to the point of either loss of surface expression or loss of glycine-gated channel activation. Unlike glycine, the unconventional agonist ivermectin forgoes the ECD, and activates the GlyR channel by binding to the TMD. It can

DOI: 10.1021/acschemneuro.5b00298
ACS Chem. Neurosci. 2016, 7, 339−348

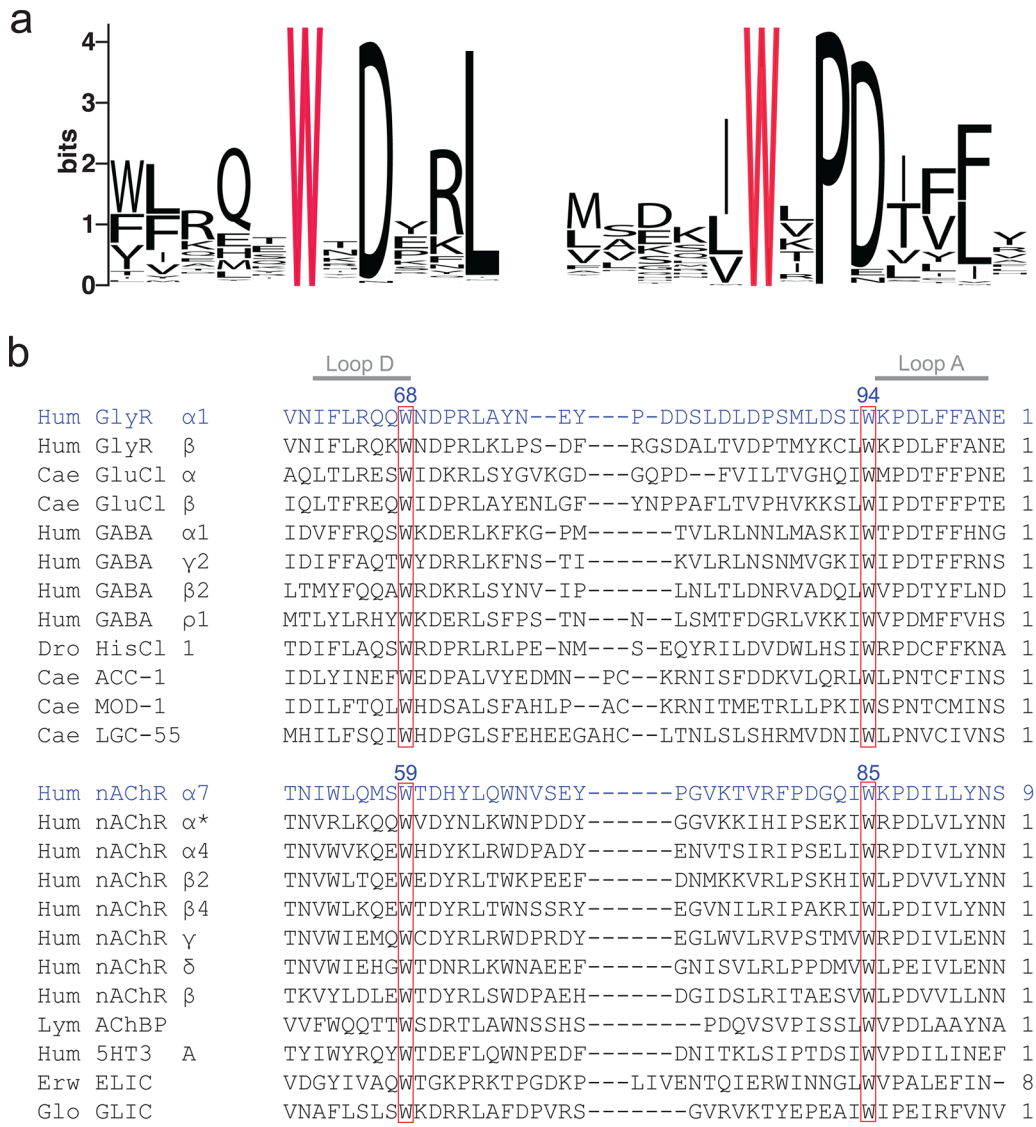

Figure 2. Two Trp residues in the extracellular domain of Cys-loop receptors are absolutely conserved. (a) Sequence logo of an alignment of 187 functional Cys-loop receptor subunits (full alignment in Figure S1, Supporting Information). (b) Amino acid sequence alignment of the ECDs of selected anionic (top) and cationic (bottom) Cys loop receptors. The conserved amino acids in loops A and D are highlighted in red. Hum, human; Cae, *Caenorhabditis elegans*; Dro, *Drosophila melanogaster*; Lym, *Lymnaea stagnalis*; Erw, *Erwinia chrysanthemi*; Glo, *Gloeobacter violaceus*. Alignment performed in ClustalW2. (* = Excludes 25 residues that occur between the QQ in Loop D of the human alpha nAChR subunit.)

thus be used to verify surface expression and intact channel function in glycine-insensitive receptors.[24] To test if Trp68 and Trp94 mutations simply abolished glycine-gated activation, we tested the effects of 10 μM ivermectin at each of the GlyR mutants. Ivermectin did not elicit currents at any of the mutants, nor did it enhance subsequent responses to glycine (Figure S2, Supporting Information), as is usually the case for glycine-insensitve mutants[25]). Thus, Trp68 and Trp94 mutations appear to prevent surface expression of GlyRs. To verify this conclusion, we directly analyzed surface expression of WT, Trp68Leu/Phe, and Trp94Leu/Phe mutant GlyRs using immunohistochemistry. As shown in Figure 3d, surface-expressed GlyR was clearly detected in WT-injected cells. In Trp68Phe, Trp94Phe, and Trp94Leu injected cells, no surface-expressed GlyR was detected. A relatively very small amount of surface-expressed GlyR was detected for Trp68Leu injected cells. This suggests that, indeed, the Trp68Phe and the Trp94Leu/Phe mutations result in a lack of surface expression. For Trp68Leu, however, the presence of surface receptors suggests that the absence of glycine-gated currents (Figure 3b) must also be attributed to some functional defect of surface receptors.

Probing the Role of Conserved Trp Side Chains in GlyR Function. Our experiments showed that Trp68 and Trp94 mutations preclude or drastically reduce functional surface expression, and certainly in the case of Trp68,[18] trafficking is obsolete in the absence of the Trp side chain. In order to probe for a role of these residues in the function of mature GlyRs, we turned to the in vivo nonsense suppression method, which enables the introduction of more subtle Trp analogues than Phe and Leu. In particular, we sought to determine if Trp hydrogen bonding ability or the location of Trp π electrons is involved in GlyR function.

To this end, we introduced a series of increasingly fluorinated Trp analogues that have different distributions of π electrons and thus, when incorporated into a receptor can incrementally

DOI: 10.1021/acschemneuro.5b00298
ACS Chem. Neurosci. 2016, 7, 339−348

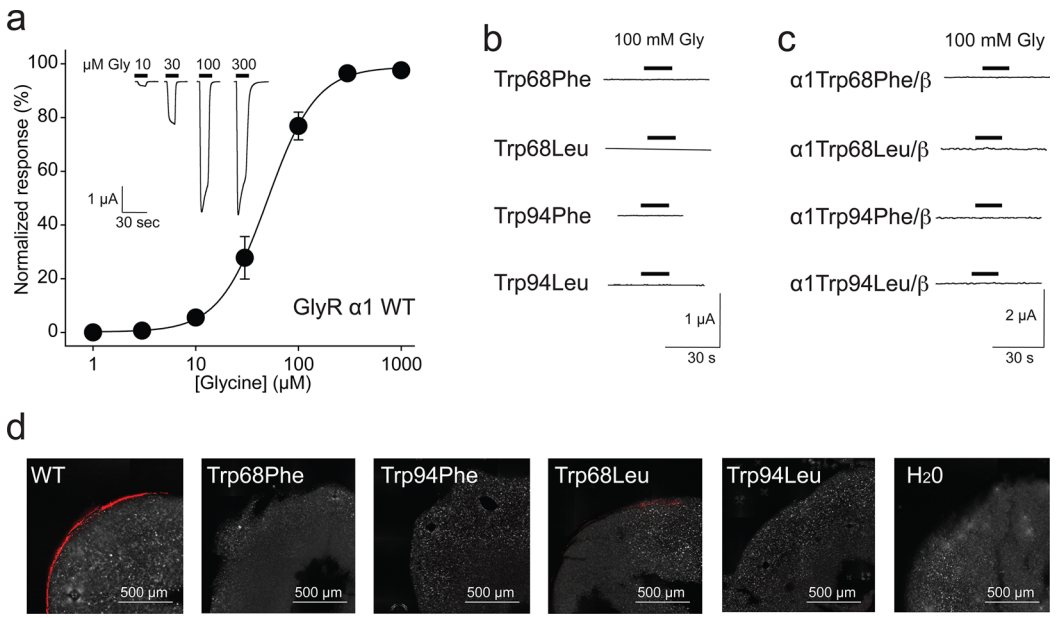

Figure 3. Electrophysiological and immunohistochemical analysis of conventional mutant GlyRs. (a) Averaged current responses of oocytes injected with WT GlyR α1 mRNA to increasing concentrations of glycine, as measured by two electrode voltage clamp (±SEM, n = 11). Inset shows an example oocyte/experiment. (b) Representative experiments on oocytes injected with indicated mutant GlyR α1 mRNAs, showing no response to application of 100 mM glycine (n = 5–6). (c) Representative experiments on oocytes coinjected with indicated mutant GlyR α1 mRNAs and WT GlyR β in a 1:1 ratio, showing no response to application of 100 mM glycine (n = 5–6). (d) Immunohistochemical experiments. *Xenopus laevis* oocytes were injected with indicated GlyR mRNAs (or H_2O) and washed with anti-GlyR primary antibody (rabbit) and then Alexa 555-conjugated secondary antibody (goat anti-rabbit).

impair cation-π interactions with ligands or vicinal side chains, as reflected in electrophysiological measurements of decreased function[26,27] (Figure 4a). Furthermore, we aimed to change the position of the indole nitrogen by incorporating the isosteric Trp derivative, Ind, which cannot act as a hydrogen bond donor[28] (Figure 4a). Both in position 68 and 94, reintroduction of the native Trp side chains via the nonsense suppression method resulted in receptors that displayed WT-like properties (Figure 4b/c, Table 1), thereby validating the nonsense suppression approach at these positions. In position 68, the introduction of one or two fluorines resulted in a reduction in glycine potency (Figure 4b), shifting the EC_{50} value from 51.2 ± 1.8 μM (Trp reincorporation) nonsignificantly to 63.8 ± 14.5 (F-Trp) or significantly to 511.7 ± 59.0 μM (F_2-Trp, P < 0.001). Further fluorination, via incorporation of F_3-Trp and F_4-Trp, only resulted in small changes in glycine potency compared to F_2-Trp (Table 1). Thus, the presence of fluorine atoms bound to the Trp C6 and C7 atoms (in F_2-, F_3-, and F_4-Trp), but not C4 or C5, alters glycine sensitivity. Furthermore, the cation−π binding ability of Trp68 is not related to potency of glycine-gated activation (Table 1), as in case of a cation−π interaction with Trp68 π electrons a monotonic increase in EC_{50} would have been expected with fluorination.[29] Similarly, fluorination of Trp94 did not incrementally alter glycine-gated activation (Figure 4c), with no significant changes from the glycine EC_{50} of 70.3 ± 15.1 μM (Trp reincorporation) at F-Trp, F2-Trp or F3-Trp-incorporated receptors (Table 1). In fact, only incorporation of F_4-Trp resulted in a significant change in glycine sensitivity (245.3 ± 102.3 μM, P < 0.01). When Ind was incorporated into position 68, we observed a decrease in the Hill coefficient but no significant change in the EC_{50} value for glycine activation (Figure 4d, Table 1), suggesting that the indole nitrogen plays at most a minor role in GlyR activation. No change in glycine sensitivity was observed with Ind in position 94 (Figure 4e).

Changes in glycine potency upon Trp fluorination reveal that Trp68 and Trp94 are indeed important to mature GlyR function. Channel activation is not drastically dependent on the indole nitrogen, nor on cation-π interactions with the aromatic moiety. However, the nonlinear, but often significant changes in glycine potency upon fluorination suggest that the exact size and shape of the aromatic moiety is important to GlyR activation.

Two Trp Residues Are Important for nAChR α7 Expression. After establishing the critical role of Trp68 and Trp94 in the expression and function of the inhibitory GlyR α1, we sought to investigate the contribution of the equivalent side chains in an excitatory member of the Cys-loop receptor family. For this purpose, we chose nAChR α7, where the equivalent residues are Trp59 (Loop D) and Trp85 (Loop A). We initially used conventional mutagenesis to generate four nAChR mutants, Trp59Phe, Trp59Leu, Trp85Phe, and Trp85Leu, and injected the corresponding mRNAs into *Xenopus* oocytes. Oocytes injected with either Trp59 mutant showed no response to acetylcholine, even at very high (100 mM) concentrations (Figure 5a). Similarly, oocytes injected with Trp85Leu mRNA showed no response to acetylcholine (Figure 5a). In contrast, the Trp85Phe mutant displayed robust acetylcholine-gated currents (Figure 5), with an acetylcholine EC_{50} value of 4.6 ± 0.7 μM, representing only a minor reduction in agonist sensitivity (Table 2). This suggested that functional nAChR expression requires merely an aromatic side chain in the Loop A position, and we therefore tested Tyr and His substitutions for Trp85. However, oocytes injected with Trp85Tyr (Figure 5a) or Trp85His mRNAs did not respond to ACh application, arguing against that possibility. As Trp85 and Phe85 receptors are both functional, the indole nitrogen does

DOI: 10.1021/acschemneuro.5b00298
ACS Chem. Neurosci. 2016, 7, 339–348

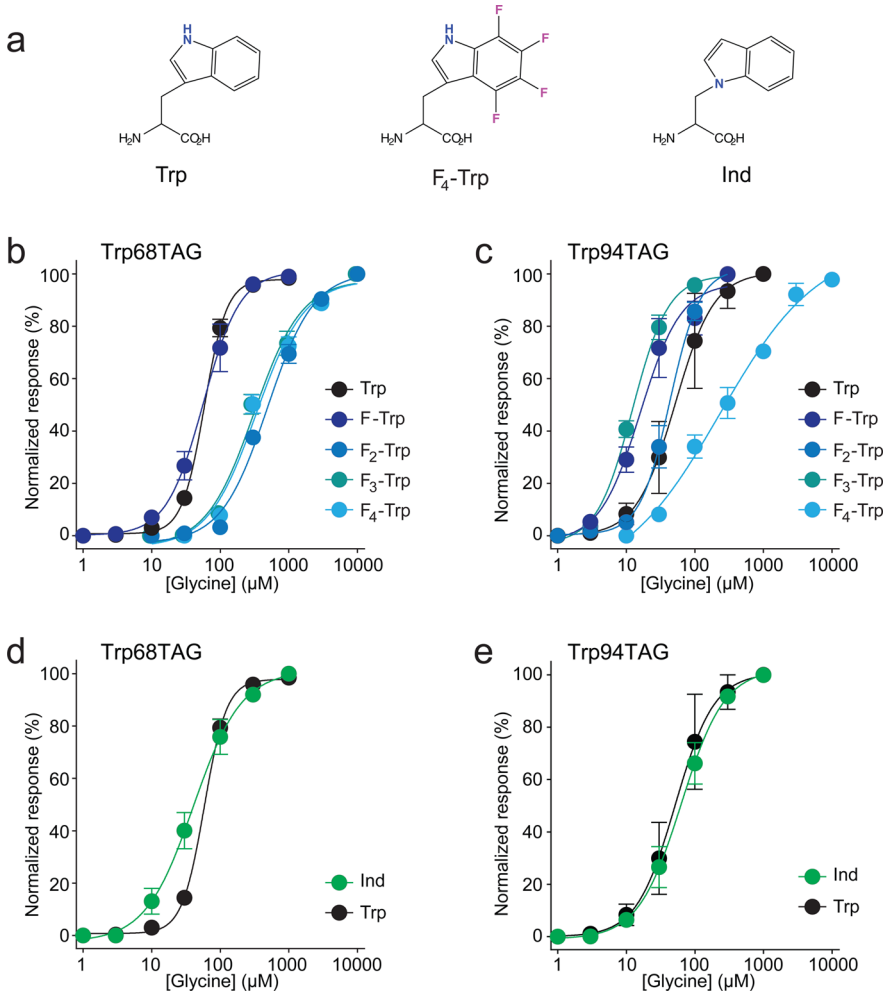

Figure 4. Incorporation of unnatural amino acids (UAAs) into the GlyR. (a) Chemical structures of Trp and selected UAAs, F_4-Trp (4,5,6,7-F_4 Trp) and Ind (2-amino-3-indol-1-yl-propionic acid). (b–e) Averaged current responses of oocytes coinjected with TAG-containing GlyR mRNA and UAA-tRNA conjugate (±SEM, $n \geq 5$ over two batches of oocytes) as measured by two electrode voltage clamp (±SEM, $n = 11$). (b) and (c) refer to fluorinated tryptophan incorporation (see inset legend for details); (d) and (e) refer to Ind incorporation. Trp-incorporated data are from the same batches of oocytes/experiments as the mutant constructs in the respective graphs.

not seem crucial to functional expression of nAChRs. In addition, as Phe85 receptors are expressed and Tyr85 receptors are not, the terminal hydroxyl moiety, as opposed to phenyl π electrons, which is similar in Tyr and Phe side chains,[30] appears to be detrimental to expression. We therefore saw no need to probe the role of these Trp properties with unnatural amino acid incorporation at the Loop A position. Furthermore, a previous study has shown that the incorporation of halogenated tryptophan analogues into the equivalent Loop A position of muscle-type nAChRs has little effect on activation by acetylcholine.[29]

In contrast, although conventional mutagenesis at the Loop D position implicated Trp59 in expression, conventional mutagenesis was unsuitable for probing function of mature receptors, as neither conventional mutant showed responses to acetylcholine. To generate functional receptors with more subtly altered properties at position 59, we therefore incorporated the fluorinated Trp analogues described above. Mono- and difluorinated Trp analogs were indeed tolerated at this position, and were activated by acetylcholine with EC_{50} values of 1.0 ± 0.1 and 1.3 ± 0.2 μM, respectively (Figure S3, Table 2). This was not significantly different from Trp-incorporated receptors, with an EC_{50} value of 0.9 ± 0.1 μM (which, in turn, showed no significant difference to WT nAChRs, EC_{50} = 2.1 ± 0.3 μM, Table 1). Unfortunately, function could not be measured with receptors containing F_3-Trp, F_4-Trp or Ind, as we failed to observe any inward currents, even at very high agonist concentrations. However, as GlyR EC_{50} values were significantly altered by either F-Trp or F_2-Trp substitutions (Table 1) and these nAChR EC_{50} values were not (Table 2), we tentatively interpret this as evidence against a role for nAChR Trp59 electrostatics in channel activation. This leads us to conclude that Trp59 does not play a major role in the function of the receptor, although a Trp (or Trp-like) side chain is crucial for expression of the receptor. Thus, and although we could not test the effects of higher fluorinated Trp derivatives at position 59, the nAChR data suggest that both Trp59 and Trp85 are integral to surface expression of nAChRs and hint that channel activation is rather independent of the unique properties of Trp at these positions.

MD Simulations Reflect the Requirement of Trp Side Chains for GlyR Function. Similar to a recent study using MD simulations to probe agonist and antagonist binding in a GluCl-based homology model of GlyR α1 with unprecedented detail,[31] we used the recently published single particle EM GlyR α1 structure[11] to conduct MD simulations. Specifically, we took

DOI: 10.1021/acschemneuro.5b00298
ACS Chem. Neurosci. 2016, 7, 339–348

Table 1. Results for Glycine-Evoked Current Recordings after Incorporation of Amino Acids with the Nonsense Suppression Method[a]

GlyR α1 construct	EC_{50} (μM)	n_H	n
WT	56.3 ± 9.1	2.6 ± 0.2	11
Trp68TAG + Trp	51.2 ± 1.8	3.1 ± 0.2*	7
Trp68TAG + F-Trp	63.8 ± 14.5	2.0 ± 0.3***	6
Trp68TAG + F_2-Trp	511.7 ± 59.0***	1.3 ± 0.1***	6
Trp68TAG + F_3-Trp	380.0 ± 95.1**	1.3 ± 0.2***	5
Trp68TAG + F_4-Trp	384.7 ± 98.7**	1.3 ± 0.1***	6
Trp68TAG + Ind	48.2 ± 11.7	1.6 ± 0.4**	7
Trp94TAG + Trp	70.3 ± 15.1	2.2 ± 0.1	6
Trp94TAG + F-Trp	15.3 ± 3.9	1.2 ± 0.3*	4
Trp94TAG + F_2-Trp	43.8 ± 7.7	2.1 ± 0.1	3
Trp94TAG + F_3-Trp	12.8 ± 1.2	1.7 ± 0.2	4
Trp94TAG + F_4-Trp	245.3 ± 102.3**	0.6 ± 0.1***	3
Trp94TAG + Ind	74.2 ± 17.4	2.0 ± 0.2	8

[a]Displayed are values of concentration for half-maximal activation (EC_{50}), Hill coefficient (n_H), and number of experiments (n). Trp analogue-incorporated constructs were compared to Trp rescue experiments (Trp68TAG + Trp or Trp94TAG + Trp) for the respective positions by one-way ANOVA with Tukey's multiple comparison test (*P < 0.05; **P < 0.01; ***P < 0.001).

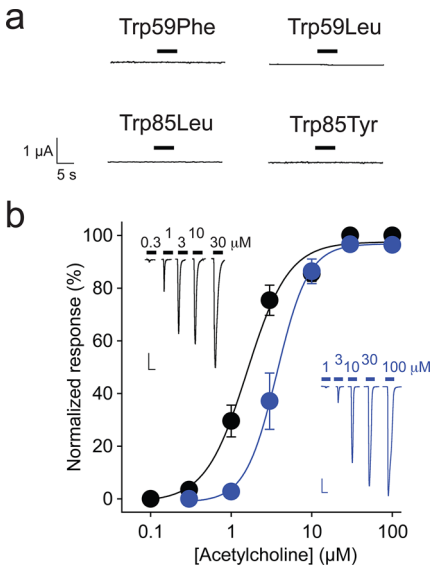

Figure 5. Electrophysiological analysis of conventional mutant nAChRs. (a) Representative recordings at oocytes injected with indicated mutant nAChR α7 mRNAs; bars indicate application of 10 mM acetylcholine. No response was observed at ≥6 oocytes for each construct over two batches of oocytes. (b) Averaged current responses to increasing acetylcholine concentrations at oocytes injected with WT (black) or Trp85Phe (blue) nAChR α7 mRNA (±SEM, n = 11). Inset figures show representative individual experiments (scale bars: WT 5 s and 0.3 μA; Trp85Phe 5 s and 2 μA).

Table 2. Results for Acetylcholine-Evoked Current Recordings after Conventional Mutagenesis or Incorporation of Amino Acids with the Nonsense Suppression Method[a]

nAChR α7 construct	EC_{50} (μM)	n_H	n
WT	2.1 ± 0.3	2.0 ± 0.2	12
Trp85Phe	4.6 ± 0.7*	3.4 ± 0.4*	9
Trp59TAG + Trp	0.9 ± 0.1	2.3 ± 0.4	6
Trp59TAG + F-Trp	1.0 ± 0.1	2.2 ± 1.0	4
Trp59TAG + F_2-Trp	1.3 ± 0.2	1.8 ± 0.4	6

[a]Displayed are values of concentration for half-maximal activation (EC_{50}), Hill coefficient (n_H), and number of experiments (n). Asterisks indicate statistical significance compared to WT (for Trp85Phe; Student's t test; *P < 0.05) or compared to Trp rescue experiment (Trp59TAG + Trp) for Trp analogue-incorporated constructs (one-way ANOVA with Tukey's multiple comparison test).

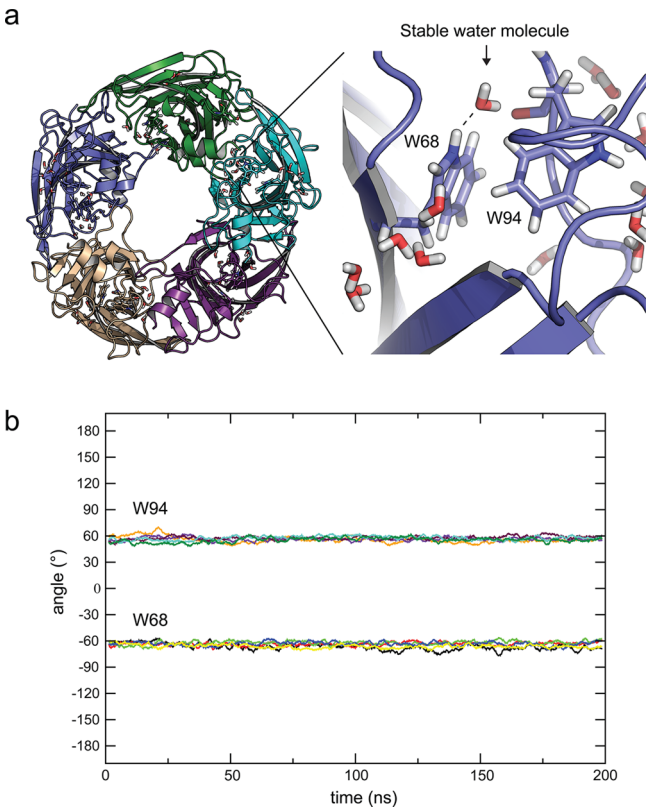

Figure 6. MD simulations on the Trp side chains and their environment in the GlyR α1 structure (3JAE). (a) MD simulation suggests an interaction between the indole nitrogen of Trp68 and a stable water molecule in one of the subunits. (b) Simulation of Trp68 and Trp94 χ1,2 dihedral angles over a 150 ns time window hints at significantly reduced conformational flexibility of the conserved Trp residues. The five GlyR α1 subunits are marked by different colors.

advantage of the approach to assess the immediate environment of the two conserved Trp side chains in the GlyR α1. We found that the conformation of the Trp pairs was very stable, facilitated by a hydrogen bond between the indole nitrogen of Trp68 and the backbone oxygen of Trp94. Interestingly, in one subunit, we found the simulations to suggest a hydrogen bond between the indole nitrogen of Trp68 and a stable water molecule that may help to position and orient the side chain (Figure 6a), a fact that may reflect the reduced Hill coefficient with the incorporation of the unnatural amino acid Ind into position 68 of the GlyR α1. Further, in support of the notion that the tryptophan pairs contribute stability to the ECD, our MD simulations showed virtually no side chain movement/rotation of these residues over the experimentally assessed time course (Figure 6b). We observed similar behavior in the simulation trajectories of our previous homology models.

Trp Residues in Cys-Loop Receptor Expression. Substitution of Loop D or A Trp residues for conventional amino acids abolished agonist-gated currents in nAChRs and

DOI: 10.1021/acschemneuro.5b00298
ACS Chem. Neurosci. 2016, 7, 339−348

GlyRs in nine of ten cases; the only exception was the Trp85Phe (Loop A) nAChR. This suggested that cell surface expression of Cys-loop receptors specifically requires a Trp side chain at these positions. This was experimentally confirmed for GlyRs, where none of the mutants were detected to the extent of WT GlyRs at the oocyte surface, unlike WT GlyRs, which were abundantly detected.

GlyR α subunits form functional homopentamers, whereas β subunits do not.[23] Chimeric α subunits, containing small segments of β subunit sequence in the ECD, are also incapable of forming functional homopentamers unless particular α-specific amino acids are reintroduced into those segments.[32] One example is an Asp-Ser pair of residues in α subunits (Lys-Cys in β subunits), only two positions upstream of the Loop A WXPD motif. The presence of this Asp-Ser pair allows an $\alpha-\beta$ chimeric subunit to form functional homopentamers alone or assemble functional heteropentamers with WT α subunits.[32] In contrast, the Lys-Cys pair precludes the expression of functional homomers and apparently even prevents the expression of subunits that can coassemble with WT subunits.[32] It is easy to imagine that the β subunit Lys-Cys pair prevents expression of a functional subunit by inducing an inappropriate Loop A conformation, including an altered orientation of the Loop A Trp. Our MD simulations suggest that such a conformational change is incompatible with the structure of a functional receptor. According to our electrophysiological experiments, the presence of WT β subunits did not confer any function to the mutated α subunits. This provides further evidence that the Trp side chains are necessary for the formation of structurally intact subunits, as even mutant α subunits of low agonist sensitivity are known to assemble functional heteromers with WT β subunits.[22] In the case of the Loop D Trp, this is reiterated by the result that Trp68Cys mutant subunits are trafficked more to the Golgi apparatus than to the cell surface.[18] Interestingly, that recent study suggests that mutations of Loop D Trp or of the downstream Asp in the Loop D WXD motif are both recognized by control apparati after leaving the endoplasmic reticulum, as opposed to mutations to other parts of the receptor that result in endoplasmic reticulum retention.[18]

Regarding nAChRs, receptor expression was not probed with immunohistochemistry, but oocytes injected with all conventional mutant mRNAs, with the exception of Trp85Phe, showed no responses to acetylcholine in electrophysiological experiments, suggesting that excitatory nAChRs also rely on the Loop D Trp side chain for appropriate expression. Although the Loop A Trp85Phe nAChR was functional, indicating that a Trp side chain is not an absolute requirement in Loop A, Tyr85 and His85 substitutions were not tolerated. Thus, the Loop A position is also very sensitive to mutation in both anion- and cation-selective Cys-loop receptors, explaining the high level of conservation at both Trp positions. Indeed, among functionally not yet characterized Cys-loop receptor subunits, we found only three examples of divergence from Trp at these positions to either Phe or Tyr (see Uniprot ID E3CTP9, Q9W4G1, Q9VVH4).

Trp Residues in Cys-Loop Receptor Function. The deleterious effects of Loop D/A Trp mutations on receptor expression make it difficult to probe the role of these side chains in characteristic Cys-loop receptor functions such as ligand-gated channel activation. Thus, the possible functional role of two uniquely conserved residues in close proximity to the ligand-binding site remains unknown. To circumvent the deleterious effects on expression and to probe function more subtly, we incorporated unnatural Trp analogues at these positions. Such analogues can be used to probe cation$-\pi$ interactions with Trp π electrons and hydrogen bonds with the Trp indole nitrogen.[26,33] Although fluorination of Trp68 and Trp94 in the GlyR caused marked changes to GlyR activation, the changes in activation were not correlated to π electron density of either Trp68 or Trp94, and were more correlated to the presence of fluorine atoms at the distal part of the Trp68 side chain. Examining the recent GlyR α1 and α3 structures (refs 11 and 14; PDB IDs 3JAE and 5CFB, respectively), it is easy to imagine that the addition of fluorine atoms to either the Trp68 or Trp94 side chain (same numbering in the GlyR α3) would disrupt what appears to be an edge-to-face (Loop A Trp-to-Loop D Trp) arrangement.[34] The alteration of this otherwise stable tryptophan pair could in turn alter the conformation of Loops A and D, which are directly involved in ligand-binding, thus altering ligand-induced receptor activation.[35]

Incorporation of Trp derivatives into the nAChR (which was only performed at the Loop D Trp59 position) caused no change in acetylcholine-gated activation. This tentatively suggests that, in mature nAChRs, the side chain properties of the Loop D Trp are not crucial to receptor function, contrasting our findings with the GlyR. Perhaps this difference relates to the fact that in amino acid-gated, anion-selective receptors, a terminal moiety of the agonist glutamate or glycine is oriented directly toward Loop D of the complementary ligand-binding face.[13,36] By contrast, in nAChR-related, amine-binding receptors, the equivalent terminal moiety is oriented more toward Loop E,[17,37] perhaps somewhat alleviating the reliance of the receptor on Loop D structure.

CONCLUSIONS

Focusing on the most uniquely conserved residues in the Cys-loop receptor ECD has revealed that at both positions, the Trp residue is required or at least strongly favored for cell surface expression across different receptors. In contrast, different Cys-loop receptors may differ in their use of these Trp side chains for agonist-gated activation. These results add a structural insight into the implication of the Loop D Trp in GlyR-related disease.[18,38] In agreement with Hassaine et al.,[12] we conclude that a pair of tryptophans at the top of the Cys-loop receptor ECD is crucial to stability and structural integrity, with mutations affecting both receptor expression and function.

METHODS

Molecular Biology. All human GlyR α1 and β constructs were in the pGEMHE vector and contained the C41A mutation (which removes the only extracellular Cys side chain, but has no effect on receptor function or pharmacology[39]); all nAChR α7 constructs were in pAMV and contained the L247T mutation to reduce desensitization.[40] nAChR α7 constructs were coexpressed with hRIC-3 cDNA in pGEM (a generous gift from Dr. M. Treinin, Hebrew University).[41] All mutants were generated using standard site-directed mutagenesis, followed by sequencing of the entire coding region. mRNA for oocyte injection was generated with the T7 mMessage mMachine kit (Ambion, Austin, TX). Oocytes (stage V–VI) from female *Xenopus laevis* frogs were prepared by collagenase treatment in OR2 (in mM: 82.5 NaCl, 2 KCl, 1 $MgCl_2$, 5 HEPES, pH 7.4) and injected with 50 nL of mRNA alone or mRNA plus tRNA (see Unnatural Amino Acid Incorporation, below). After an incubation at 18 °C for 12–72 h, oocytes were used for electrophysiological recordings or immunohistochemical analysis.

DOI: 10.1021/acschemneuro.5b00298
ACS Chem. Neurosci. 2016, 7, 339–348

Unnatural Amino Acid Incorporation. The principle of the in vivo nonsense suppression methodology for unnatural amino acid (UAA) incorporation is outlined elsewhere.[33] Briefly, the amine of the UAAs 2-amino-3-indol-1-yl-propionic acid (Ind) and fluorinated Trp derivatives (4,5,6,7-F_4-Trp) (all prepared as previously described[27]) was protected with nitroveratryloxycarbonyl (NVOC). For coupling to the dinucleotide dCA (Dharmacon, Lafayette, CO), the carboxyl group was activated as the cyanomethyl ester. After storage in DMSO (−80 °C), the product was ligated to a modified (G73) *Tetrahymena thermophila* tRNA (synthesized using an oligonucleotide (Integrated DNA Technologies) as a template). Immediately before coinjection with the mutated receptor mRNA, the (NVOC) protection group of the aminoacylated tRNA-UAA was removed by 400 W UV irradiation for 55 s. Typically, we coinjected 10−80 ng of tRNA-UAA and 25−50 ng of mutated receptor mRNA containing an amber stop codon (TAG) at the position of interest, in a total volume of 50 nL. tRNA coupled to dCA alone (i.e., with no appended UAA) was coinjected with the TAG-mutated receptor mRNA, and these oocytes were recorded in parallel to all other experiments as a control for nonspecific incorporation of endogenous amino acids. In such control experiments, we did not observe any detectable currents at all GlyR and nAChR constructs, even with high (100 mM) agonist concentrations, suggesting negligible levels of nonspecific incorporation.

Electrophysiology. Two-electrode voltage-clamp recordings were conducted using a custom-made recording chamber and an automated perfusion system (AutoMate Scientific). Glass capillaries with a resistance of 0.5−1 MΩ were backfilled with 3 M KCl and cells were voltage-clamped at a holding potential of −40 mV (GlyR α1) and −80 mV (nAChR α7), respectively. ND96 (in mM: 96 NaCl, 2 KCl, 1 $MgCl_2$, 1.8 $CaCl_2$, 5 HEPES, pH 7.4) was used for electrophysiological recordings. Currents were recorded using an OC-725C amplifier (Warner Instruments), and data was acquired at 200 Hz with an Axon Digidata 1550 digitizer (Molecular Devices). Offline data analysis was conducted using Clampex 10.5.1.0 software (Molecular Devices), and signals were digitally filtered at 2 Hz for analysis and display. The empirical Hill equation, fitted with a nonlinear least-squares algorithm, was used to obtain half-maximal concentrations (EC_{50}) and Hill coefficient (n_H) values for ligand-induced activation. All results are expressed as means ± SEM of three or more independent experiments from at least two batches of oocytes.

Immunohistochemistry. The procedure was adapted from a recent study.[42] Two days after mRNA injection, oocytes were fixed in a 3.7% solution of *p*-formaldehyde in phosphate buffered saline (PBS, 0.01 M: 137 mM NaCl, 2.7 mM KCl, 10 mM Na_2HPO_4, 1.8 mM KH_2PO_4, pH 7.4) for 3 h and washed in a 1% (w/v) solution of bovine serum albumin (BSA) in the same buffer (3 × 10 min) at room temperature. Oocytes were incubated overnight in a polyclonal rabbit anti-GlyR antibody (ThermoFisher Scientific catalog number PA1-4661) diluted 1:1000 in wash buffer. On the following day, oocytes were washed in 1% BSA/PBS and incubated with a goat anti-rabbit IgG secondary antibody conjugated with Alexa Fluor 555 (ThermoFisher Scientific catalog number A27039) diluted 1:500 at RT for 3 h (all antibody dilutions in 1% BSA/PBS). After washing in 1% BSA/PBS, oocytes were quick-frozen in isopentane and sectioned into 50 μm slices with a CM3050 S cryostat (Leica). Slices were mounted in 70% glycerol in PBS on adhesive microscope slides and imaged with a Zeiss LSM 710 laser scanning confocal microscope equipped with a 20×, 0.8 NA Plan-Apochromat objective and two photomultiplier tubes. Alexa Fluor 555 was excited at 561 nm, and fluorescence data was collected from 570 to 750 nm.

Sequence Alignment. All sequence alignments were performed with ClustalW2,[43] and the entire sequence alignment for loops A and D is shown in Figure S1. The sequence logo in Figure 2 was generated using WebLogo.[44]

Molecular Dynamics Simulations. Analysis of our previously reported simulation of human GlyR1[31] suggested that this Trp pair was conformationally stable. During our analysis, structures for the α1 glycine receptor from *Danio rerio* were solved by single particle cryo-electron microscopy[11] as well as a crystal structure for the human α3 glycine receptor[14] were determined. We thus performed MD simulations of the extracellular domain (ECD) only (for expediency) of the α1 GlyR in complex with glycine (PDB: 3JAE) to investigate the behavior of this Trp pair. We used the Amber 12 package[45] with the ff12SB force field. Missing side chain atoms were added with the xleap module of AMBER. The ECD was solvated with an octagonal box of TIP3P water molecules and neutralized using Na^+. Minimization was performed in two steps. First, only the water molecules and ions were minimized with 1000 steps of steepest descent minimization and 1000 steps of conjugate gradient minimization. Second, the restraints on the protein were removed and the whole system was relaxed with 3000 steps of steepest descent minimization and 3000 steps of conjugate gradient minimization. The cutoff of the nonbonded interactions was set to 12 Å for the energy minimization process. After minimization, MD was performed. Initially, the solute was restrained and the whole system was gradually heated from 10 to 300 K in 100 ps in the NVT ensemble. Then the system was equilibrated in the NPT ensemble where the temperature and pressure were kept at 300 K and 1 atm, respectively. Finally, in the production process, the whole system was relaxed and a 50 ns molecular dynamics run was carried out. For all MD steps, the time step was set to 0.002 ps, the particle mesh Ewald (PME) method[46] was applied to deal with long-range electrostatic interactions, and the lengths of the bonds involving hydrogen atoms were fixed with the SHAKE algorithm.[47]

■ ASSOCIATED CONTENT

Supporting Information

The Supporting Information is available free of charge on the ACS Publications website at DOI: 10.1021/acschemneuro.5b00298.

Sequence alignment of 187 Cys-loop receptors, GlyR activation by ivermectin, and fluorination of Trp59 in nAChR α7 (PDF)

■ AUTHOR INFORMATION

Present Address

[§]R.Y.: Key Laboratory of Marine Drugs, Chinese Ministry of Education, School of Medicine and Pharmacy, Ocean University of China, Qingdao 266003, China.

Author Contributions

N.B.: designed and conducted experiments (other than the MD simulations). T.L.: designed experiments and wrote the manuscript. R.Y.: conducted MD simulations. P.C.B.: designed experiments and wrote the manuscript. S.A.P.: designed experiments and wrote the manuscript.

Funding

N.B.: German National Academic Foundation. T.L.: Lundbeck Foundation and the The Danish Council for Independent Research. R.Y. and P.C.B: This work was supported by MRC grant MR/J007110/1. S.A.P.: Center for Biopharmaceuticals (University of Copenhagen), the Carlsberg Foundation and the Lundbeck Foundation.

Notes

The authors declare no competing financial interest.

■ ACKNOWLEDGMENTS

This project made use of time on ARCHER granted via the UK High-End Computing Consortium for Biomolecular Simulation, HECBioSim (hecbiosim.ac.uk), supported by EPSRC (Grant No. EP/L000253/1)

■ ABBREVIATIONS

ECD, extracellular domain; EC_{50}, agonist concentration required for half-maximal activation; GlyR, glycine receptor;

DOI: 10.1021/acschemneuro.5b00298
ACS Chem. Neurosci. 2016, 7, 339−348

nAChR, nicotinic acetylcholine receptor; TMD, transmembrane domain; WT, wild type; WX(P)D, amino acid sequence motif in which W stands for tryptophan, X for any amino acid, P for proline and D for aspartic acid

REFERENCES

(1) Hille, B. (2001) *Ion channels of excitable membranes*, 3rd ed., Sinauer, Sunderland, MA.

(2) Miller, P. S., and Smart, T. G. (2010) Binding, activation and modulation of Cys-loop receptors. *Trends Pharmacol. Sci. 31*, 161−174.

(3) Ashcroft, F. M. (2006) From molecule to malady. *Nature 440*, 440−447.

(4) Dineley, K. T., Pandya, A. A., and Yakel, J. L. (2015) Nicotinic ACh receptors as therapeutic targets in CNS disorders. *Trends Pharmacol. Sci. 36*, 96−108.

(5) Korpi, E. R., and Sinkkonen, S. T. (2006) GABA(A) receptor subtypes as targets for neuropsychiatric drug development. *Pharmacol. Ther. 109*, 12−32.

(6) Tsetlin, V. I. (2015) Three-finger snake neurotoxins and Ly6 proteins targeting nicotinic acetylcholine receptors: pharmacological tools and endogenous modulators. *Trends Pharmacol. Sci. 36*, 109−123.

(7) Brejc, K., van Dijk, W. J., Klaassen, R. V., Schuurmans, M., van Der Oost, J., Smit, A. B., and Sixma, T. K. (2001) Crystal structure of an ACh-binding protein reveals the ligand-binding domain of nicotinic receptors. *Nature 411*, 269−276.

(8) Karlin, A., and Akabas, M. H. (1995) Toward a structural basis for the function of nicotinic acetylcholine receptors and their cousins. *Neuron 15*, 1231−1244.

(9) Miyazawa, A., Fujiyoshi, Y., and Unwin, N. (2003) Structure and gating mechanism of the acetylcholine receptor pore. *Nature 423*, 949−955.

(10) Althoff, T., Hibbs, R. E., Banerjee, S., and Gouaux, E. (2014) X-ray structures of GluCl in apo states reveal a gating mechanism of Cys-loop receptors. *Nature 512*, 333−337.

(11) Du, J., Lu, W., Wu, S., Cheng, Y., and Gouaux, E. (2015) Glycine receptor mechanism elucidated by electron cryo-microscopy. *Nature 526*, 224−229.

(12) Hassaine, G., Deluz, C., Grasso, L., Wyss, R., Tol, M. B., Hovius, R., Graff, A., Stahlberg, H., Tomizaki, T., Desmyter, A., Moreau, C., Li, X. D., Poitevin, F., Vogel, H., and Nury, H. (2014) X-ray structure of the mouse serotonin 5-HT3 receptor. *Nature 512*, 276−281.

(13) Hibbs, R. E., and Gouaux, E. (2011) Principles of activation and permeation in an anion-selective Cys-loop receptor. *Nature 474*, 54−60.

(14) Huang, X., Chen, H., Michelsen, K., Schneider, S., and Shaffer, P. L. (2015) Crystal structure of human glycine receptor-alpha3 bound to antagonist strychnine. *Nature 526*, 277−280.

(15) Miller, P. S., and Aricescu, A. R. (2014) Crystal structure of a human GABAA receptor. *Nature 512*, 270−275.

(16) Lynagh, T., and Pless, S. A. (2014) Principles of agonist recognition in Cys-loop receptors. *Front. Physiol. 5*, 160.

(17) Celie, P. H., van Rossum-Fikkert, S. E., van Dijk, W. J., Brejc, K., Smit, A. B., and Sixma, T. K. (2004) Nicotine and carbamylcholine binding to nicotinic acetylcholine receptors as studied in AChBP crystal structures. *Neuron 41*, 907−914.

(18) Schaefer, N., Kluck, C. J., Price, K. L., Meiselbach, H., Vornberger, N., Schwarzinger, S., Hartmann, S., Langlhofer, G., Schulz, S., Schlegel, N., Brockmann, K., Lynch, B., Becker, C. M., Lummis, S. C., and Villmann, C. (2015) Disturbed neuronal ER-Golgi sorting of unassembled glycine receptors suggests altered subcellular processing is a cause of human hyperekplexia. *J. Neurosci. 35*, 422−437.

(19) Spier, A. D., and Lummis, S. C. (2000) The role of tryptophan residues in the 5-Hydroxytryptamine(3) receptor ligand binding domain. *J. Biol. Chem. 275*, 5620−5625.

(20) Srinivasan, S., Nichols, C. J., Lawless, G. M., Olsen, R. W., and Tobin, A. J. (1999) Two invariant tryptophans on the alpha1 subunit define domains necessary for GABA(A) receptor assembly. *J. Biol. Chem. 274*, 26633−26638.

(21) Dougherty, D. A. (2013) The cation-pi interaction. *Acc. Chem. Res. 46*, 885−893.

(22) Chung, S. K., Vanbellinghen, J. F., Mullins, J. G., Robinson, A., Hantke, J., Hammond, C. L., Gilbert, D. F., Freilinger, M., Ryan, M., Kruer, M. C., Masri, A., Gurses, C., Ferrie, C., Harvey, K., Shiang, R., Christodoulou, J., Andermann, F., Andermann, E., Thomas, R. H., Harvey, R. J., Lynch, J. W., and Rees, M. I. (2010) Pathophysiological mechanisms of dominant and recessive GLRA1 mutations in hyperekplexia. *J. Neurosci. 30*, 9612−9620.

(23) Lynch, J. W. (2004) Molecular structure and function of the glycine receptor chloride channel. *Physiol. Rev. 84*, 1051−1095.

(24) Lynagh, T., and Lynch, J. W. (2010) An improved ivermectin-activated chloride channel receptor for inhibiting electrical activity in defined neuronal populations. *J. Biol. Chem. 285*, 14890−14897.

(25) Lynagh, T., Webb, T. I., Dixon, C. L., Cromer, B. A., and Lynch, J. W. (2011) Molecular determinants of ivermectin sensitivity at the glycine receptor chloride channel. *J. Biol. Chem. 286*, 43913−43924.

(26) Van Arnam, E. B., and Dougherty, D. A. (2014) Functional probes of drug-receptor interactions implicated by structural studies: Cys-loop receptors provide a fertile testing ground. *J. Med. Chem. 57*, 6289−6300.

(27) Pless, S. A., Galpin, J. D., Niciforovic, A. P., and Ahern, C. A. (2011) Contributions of counter-charge in a potassium channel voltage-sensor domain. *Nat. Chem. Biol. 7*, 617−623.

(28) Pless, S. A., Galpin, J. D., Niciforovic, A. P., Kurata, H. T., and Ahern, C. A. (2013) Hydrogen bonds as molecular timers for slow inactivation in voltage-gated potassium channels. *eLife 2*, e01289.

(29) Zhong, W., Gallivan, J. P., Zhang, Y., Li, L., Lester, H. A., and Dougherty, D. A. (1998) From ab initio quantum mechanics to molecular neurobiology: a cation-pi binding site in the nicotinic receptor. *Proc. Natl. Acad. Sci. U. S. A. 95*, 12088−12093.

(30) Mecozzi, S., West, A. P., Jr., and Dougherty, D. A. (1996) Cation-pi interactions in aromatics of biological and medicinal interest: electrostatic potential surfaces as a useful qualitative guide. *Proc. Natl. Acad. Sci. U. S. A. 93*, 10566−10571.

(31) Yu, R., Hurdiss, E., Greiner, T., Lape, R., Sivilotti, L., and Biggin, P. C. (2014) Agonist and antagonist binding in human glycine receptors. *Biochemistry 53*, 6041−6051.

(32) Griffon, N., Buttner, C., Nicke, A., Kuhse, J., Schmalzing, G., and Betz, H. (1999) Molecular determinants of glycine receptor subunit assembly. *EMBO journal 18*, 4711−4721.

(33) Pless, S. A., and Ahern, C. A. (2013) Unnatural amino acids as probes of ligand-receptor interactions and their conformational consequences. *Annu. Rev. Pharmacol. Toxicol. 53*, 211−229.

(34) Guvench, O., and Brooks, C. L., 3rd. (2005) Tryptophan side chain electrostatic interactions determine edge-to-face vs parallel-displaced tryptophan side chain geometries in the designed beta-hairpin "trpzip2". *J. Am. Chem. Soc. 127*, 4668−4674.

(35) Corringer, P. J., Poitevin, F., Prevost, M. S., Sauguet, L., Delarue, M., and Changeux, J. P. (2012) Structure and pharmacology of pentameric receptor channels: from bacteria to brain. *Structure 20*, 941−956.

(36) Pless, S. A., Millen, K. S., Hanek, A. P., Lynch, J. W., Lester, H. A., Lummis, S. C., and Dougherty, D. A. (2008) A cation-pi interaction in the binding site of the glycine receptor is mediated by a phenylalanine residue. *J. Neurosci. 28*, 10937−10942.

(37) Kesters, D., Thompson, A. J., Brams, M., van Elk, R., Spurny, R., Geitmann, M., Villalgordo, J. M., Guskov, A., Danielson, U. H., Lummis, S. C., Smit, A. B., and Ulens, C. (2013) Structural basis of ligand recognition in 5-HT3 receptors. *EMBO Rep. 14*, 49−56.

(38) Tsai, C. H., Chang, F. C., Su, Y. C., Tsai, F. J., Lu, M. K., Lee, C. C., Kuo, C. C., Yang, Y. W., and Lu, C. S. (2004) Two novel mutations of the glycine receptor gene in a Taiwanese hyperekplexia family. *Neurology 63*, 893−896.

(39) Pless, S. A., Dibas, M. I., Lester, H. A., and Lynch, J. W. (2007) Conformational variability of the glycine receptor M2 domain in

DOI: 10.1021/acschemneuro.5b00298
ACS Chem. Neurosci. 2016, 7, 339−348

response to activation by different agonists. *J. Biol. Chem. 282*, 36057−36067.
(40) Revah, F., Bertrand, D., Galzi, J. L., Devillers-Thiery, A., Mulle, C., Hussy, N., Bertrand, S., Ballivet, M., and Changeux, J. P. (1991) Mutations in the channel domain alter desensitization of a neuronal nicotinic receptor. *Nature 353*, 846−849.
(41) Williams, M. E., Burton, B., Urrutia, A., Shcherbatko, A., Chavez-Noriega, L. E., Cohen, C. J., and Aiyar, J. (2005) Ric-3 promotes functional expression of the nicotinic acetylcholine receptor alpha7 subunit in mammalian cells. *J. Biol. Chem. 280*, 1257−1263.
(42) Rienzo, M., Lummis, S. C., and Dougherty, D. A. (2014) Structural requirements in the transmembrane domain of GLIC revealed by incorporation of noncanonical histidine analogs. *Chem. Biol. 21*, 1700−1706.
(43) Larkin, M. A., Blackshields, G., Brown, N. P., Chenna, R., McGettigan, P. A., McWilliam, H., Valentin, F., Wallace, I. M., Wilm, A., Lopez, R., Thompson, J. D., Gibson, T. J., and Higgins, D. G. (2007) Clustal W and Clustal X version 2.0. *Bioinformatics 23*, 2947−2948.
(44) Crooks, G. E., Hon, G., Chandonia, J. M., and Brenner, S. E. (2004) WebLogo: a sequence logo generator. *Genome Res. 14*, 1188−1190.
(45) Salomon-Ferrer, R., Case, D. A., and Walker, R. C. (2013) An overview of the Amber biomolecular simulation package. *Wires Comput. Mol. Sci. 3*, 198−210.
(46) Darden, T., York, D., and Pedersen, L. (1993) Particle Mesh Ewald - an N.Log(N) Method for Ewald Sums in Large Systems. *J. Chem. Phys. 98*, 10089−10092.
(47) Ryckaert, J. P., Ciccotti, G., and Berendsen, H. J. C. (1977) Numerical-Integration of Cartesian Equations of Motion of a System with Constraints - Molecular-Dynamics of N-Alkanes. *J. Comput. Phys. 23*, 327−341.

DOI: 10.1021/acschemneuro.5b00298
ACS Chem. Neurosci. 2016, 7, 339−348